Published OnlineFirst January 20, 2021; DOI: 10.1158/1541-7786.MCR-20-0462

Cross-talk between YAP and RAR-RXR Drives Expression of Stemness Genes to Promote 5-FU Resistance and Self-Renewal in Colorectal Cancer Cells

Marjolaine Bauzone[1], Mouloud Souidi[1], Anne-Frédérique Dessein[1,2], Maxence Wisztorski[3], Audrey Vincent[1], Jean-Pascal Gimeno[3], Didier Monté[4,5], Isabelle Van Seuningen[1], Christian Gespach[6], and Guillemette Huet[1,2]

ABSTRACT

The mechanisms whereby the Hippo pathway effector YAP regulates cancer cell stemness, plasticity, and chemoresistance are not fully understood. We previously showed that in 5-fluorouracil (5-FU)–resistant colorectal cancer cells, the transcriptional coactivator YAP is differentially regulated at critical transitions connected with reversible quiescence/dormancy to promote metastasis. Here, we found that experimental YAP activation in 5-FU–sensitive and 5-FU–resistant HT29 colorectal cancer cells enhanced nuclear YAP localization and the transcript levels of the retinoic acid (RA) receptors RARα/γ and RAR target genes *CYP26A1, ALDH1A3*, and *LGR5* through RA Response Elements (RARE). In these two cell models, constitutive YAP activation reinforced the expression of the stemness biomarkers and regulators ALDH1A3, LGR5, and OCT4. Conversely, YAP silencing, RAR/RXR inhibition by the pan-RAR antagonist BMS493, and vitamin A depletion downregulated stemness traits and self-renewal. Regarding the mechanisms engaged, proximity-dependent labeling, nuclear YAP pulldown coupled with mass spectrometry, and chromatin immunoprecipitation (ChIP)/re-ChIP experiments revealed: (i) the nuclear colocalization/interaction of YAP with RARγ and RXRs; and (ii) combined genomic co-occupancy of YAP, RARα/γ, and RXRα interactomes at proximal RAREs of *LGR5* and *ALDH1A3* promoters. Moreover, activation of the YAP/RAR-RXR cross-talk in colorectal cancer cells promoted RAR self-activation loops via vitamin A metabolism, RA, and active RAR ligands generated by ALDH1A3. Together, our data identify YAP as a bona fide RAR-RXR transcriptional coactivator that acts through RARE-activated stemness genes.

Implications: Targeting the newly identified YAP/RAR-RXR cross-talk implicated in cancer cell stemness maintenance may lead to multitarget combination therapies for patients with colorectal cancer.

Introduction

Retinoic acid (RA), a metabolite of retinol (vitamin A), has a major role in the regulation of stem cell proliferation/differentiation and plasticity during various aspects of fetal and postnatal developmental processes. RA is a ligand for RA receptors (RARα/β/γ) and interacts with cis-acting RA Response Elements (RARE) in target gene promoters and enhancers in distal genomic regions. Heterodimer binding to RAREs leads to recruitment of corepressor and coactivator complexes, resulting in chromatin remodeling and transcriptional activity. RXRs also form (i) nonpermissive silent heterodimers for activity in their interaction with thyroid hormone and vitamin D nuclear receptors (NR); (ii) conditional ligand-dependent heterodimers with RARs and vitamin D NRs, and (iii) permissive RXR-RXR homodimers and RXR heterodimers engaged with PPARs, LXR, and FRX NRs. These permissive RXR-NRs heterodimers remain functionally activated by their respective alternative ligands (1, 2). In acute promyelocytic leukemia, the use of *all-trans* RA (ATRA) in differentiation therapy proved to be a successful treatment strategy (3). The natural RAR ligands are ATRA and its stereoisomers 9-*cis*-RA and 13-*cis*-RA, whereas RXRs are activated by endogenous 9-*cis*-13,14-dihydroxyretinoic acid ligand (1). Besides significant effects on cell differentiation, RA also promotes reprogramming of somatic cells into induced pluripotent stem cells and sustains embryonic stem cell pluripotency (4, 5). Retinoids are also tested in the prevention and treatment of carcinomas. However, clinical trials showed only limited success in breast and non–small cell lung cancer therapy (6).

YAP-TAZ/Hippo signaling is another key mechanism in the regulation of normal stem cell expansion and organ development (7–9). Nuclear YAP activity is mostly supported by its potent coactivator function toward Transcriptional Enhanced Associate Domain (TEAD) transcription factors and is negatively regulated by the tumor-suppressive functions of Hippo pathways. The core components of Hippo comprise a cascade of Mst1/2 and Lats1/2 Serine/Threonine kinases that phosphorylates YAP at Ser-127, resulting in YAP cytoplasmic sequestration, proteasomal degradation, and nuclear exclusion (10). In the absence of active Hippo signaling, YAP/TAZ proteins can shuttle to the nucleus, where they act as potent transcriptional coactivators, mainly for TEADs. By inhibiting YAP nuclear activity, Hippo acts as sensor to many aspects of the spatial organization of cellular

[1]Université Lille, CNRS, Inserm, CHU Lille, UMR9020-UMR1277 – CANTHER – Cancer Heterogeneity, Plasticity and Resistance to Therapies, Lille, France. [2]Centre de Biopathologie, Lille CHU, Lille, France. [3]Université Lille, Inserm, CHU Lille, U1192 – Protéomique Réponse Inflammatoire Spectrométrie de Masse – PRISM, Lille, France. [4]CNRS ERL9002 Integrative Structural Biology, Lille, France. [5]Université Lille, Inserm, CHU Lille, Institut Pasteur de Lille, U1167 – RID-AGE – Risk Factors and Molecular Determinants of Aging-Related Diseases, Lille, France. [6]Sorbonne Université, Inserm U938, Team TGFβ Signaling in Cellular Plasticity and Cancer, Centre de Recherche Saint-Antoine, CRSA, Paris, France.

Note: Supplementary data for this article are available at Molecular Cancer Research Online (http://mcr.aacrjournals.org/).

M. Bauzone, M. Souidi, C. Gespach, and G. Huet contributed equally to this article.

Corresponding Author: Guillemette Huet, Laboratoire CANTHER, UMR 9020 CNRS-1277 Inserm, 1 Place de Verdun, Bâtiment Cancer, F-59045 Lille Cedex, France. Phone: 33320298867; Fax: 33320538562; E-mail: guillemette.huet@inserm.fr

Mol Cancer Res 2021;19:612–22

doi: 10.1158/1541-7786.MCR-20-0462

Published OnlineFirst January 20, 2021; DOI: 10.1158/1541-7786.MCR-20-0462

adhesions and polarity, cell shape, and mechano-transduction (11). After injury of the intestine, YAP allows epithelial regeneration through the reprogramming of Leucine-rich repeat-containing G-protein–coupled receptors (LGR5) in intestinal stem cells (12). LGR5-positive intestinal stem cells give rise to proliferating progenitors and their differentiated counterparts Paneth cells, enterocytes, goblet cells, and several enteroendocrine cell populations (13). Recent lineage tracing experiments highlighted the role of LGR5 in colorectal cancer (CRC; refs. 14, 15).

In this framework, we previously reported that human colorectal cancer cells escape 5-fluorouracil (5-FU) chemotherapy-induced cell death by entering stemness and quiescence associated with reversible downregulation of nuclear YAP. Consistently, high YAP expression correlates with colorectal cancer relapse, metastatic recurrence, and shorter patient survival following 5-FU–based chemotherapy (16, 17). In the present study, we explored the potential interplay between YAP and RAR-RXR signaling pathways on stemness maintenance in parental HT29 cells and 5-FU–resistant 5F31 counterparts. We established that a new YAP/RAR-RXR cross-talk initiated by ectopic YAP activation upregulates RA receptors and RARE-activated genes *CYP26A1, ALDH1A3*, and *LGR5*. Moreover, our study highlights the pattern of the molecular interactions between YAP and RARs (RXRα, RARα/γ) that can be associated with their dynamic genomic co-occupancy of proximal RAREs at the *ALDH1A3* and *LGR5* stemness genes promoters.

Materials and Methods

Human colorectal cancer cell lines and spheroids

HT-29 parental cell line (RRID CVCL_0320) and its clonal 5-FU–resistant subpopulation of 5F31 cells and RKO cells (RRID CVCL_0504) were cultured as previously described (16, 17). Cell lines were authenticated through the short tandem repeat DNA profile analysis according to the procedures recommended by the American Type Culture Collection Institute (latest test date on November 2019). Cells were used between second and sixth passages after thawing. Mycoplasma testing was carried out by PCR detection. HT29 cells were cultured in DMEM media containing 10% of heat-inactivated FBS and supplemented with 2 mmol/L L-glutamine and 1% penicillin–streptomycin solution. For sphere formation, cells were plated at a density of 2,000 cells/mL on plates coated with poly-2-hydroxyethyl-metacrylate (0.5 mg/mL in ethanol) and cultured in serum-free DMEM/F12 medium supplemented with 20 ng/mL bFGF, 20 ng/mL EGF, and 1x B27 supplement. The number of spheroids in ten fields was counted. Self-renewal was measured by the increased number of spheres over two generations.

Stable transfection of YAPdc and empty vectors in colorectal cancer cells

For virus production and colorectal cancer cell infection, EcoPack-293 cells (Clontech) were transfected with pLPCX-YAPdc or pLPCX empty retroviral vector (Clontech) as a control. Two days after transfection, culture media were harvested and 0.45-μm filtered. After addition of 6 μg/mL polybrene, they were added to the target cells in 6-well plates and centrifugated at 1,200 × *g* for 60 minutes at 30°C. The next day, culture media were changed, and infected cells were selected with 3 μg/mL of puromycin.

RNA extraction, qRT-PCR, immunostaining, and Western blots

Total RNA was extracted from control and YAPdc-transfected HT29, 5F31, and RKO cells using the NucleoSpin kit (Macherey-Nagel) following the manufacturer's procedures. One microgram of total RNA was reverse-transcribed with M-MLV Transcriptase (Promega). qRT-PCR was completed using the SsoFast EvaGreen Supermix kit and the CFX96 real-time PCR system (Bio-Rad). Each sample was done in duplicate or triplicate. Relative gene expression levels were normalized to the housekeeping gene *RPLP0* using the ΔΔCt method. For immunofluorescence (IF) studies, HT29 and 5F31 cells grown in Nunc Lab-Tek Chamber Slides (Thermo Fischer Scientific) were fixed at 4°C for 20 minutes with 4% (v/v) paraformaldehyde (PFA), quenched with 50 mmol/L NH_4Cl in PBS, and permeabilized for 20 minutes with 0.2% (w/v) saponin in PBS. The saturation step was done with PBS containing 3% (w/v) BSA and 0.2% saponin. Cells were incubated overnight with the primary antibody. After wash-up, labeled secondary antibodies were used (Alexa Fluor 594, Life Technologies). Nuclei were identified in Vectashield mounting media with diamidino-2-phenylindole (DAPI; Vector Laboratories). Slides were fixed in mounting medium containing DAPI and visualized with a Carl Zeiss LSM 710 confocal microscope. Images were captured and analyzed with the Zeiss Efficient Navigation Software.

Proximity ligation assay

Cells were grown on Lab-Tek chamber slides (Nunc), fixed with 4% PFA, and permeabilized with 0.2% saponin (w/v, Sigma) in the presence of 3% BSA, w/v (Sigma). Cells were incubated with anti-RARγ (H-6, Santa Cruz Biotechnology) and anti-YAP antibodies (D8H1X, Cell Signaling Technology) overnight at room temperature. Then, slides were washed 3 times in D-PBS buffer containing Mg^{++}/Ca^{++} before addition of the Duolink In Situ reagents (Olink Bioscience) as described by the manufacturer's instructions. Slides were then exposed to the mounting medium containing DAPI and visualized with a Carl Zeiss LSM 710 confocal microscope. Images were captured and analyzed with the ZEN software.

Affinity purification and LC/MS-MS analysis of nuclear YAP interactome

For affinity purification of YAP-interacting proteins, nuclear extracts were prepared as previously described (18). Briefly, YAPdc-expressing HT29 cells were lysed in hypotonic buffer (10 mmol/L Tris-HCl buffer, 1.5 mmol/L $MgCl_2$, and 10 mmol/L KCl, pH 7.65) and disrupted by 18 strokes of a Dounce homogenizer. The cytosolic fraction was separated from the pellet by centrifugation at 700 × *g* at 4°C for 10 minutes. Nuclear extracts were obtained by incubation of nuclear pellets for 30 minutes at 4°C in high-salt buffer (900 mmol/L NaCl, 20 mmol/L Tris-HCl, pH 7.65, 25% glycerol, 1.5 mmol/L $MgCl_2$, and 0.2 mmol/L EDTA) and adjusted to the final concentration of 300 mmol/L NaCl. Nuclear extracts were then sonicated with a Bioruptor Power-up (Diagenode) for 10 minutes. YAP coimmunoprecipitates were obtained by overnight incubation of nuclear extracts with the anti-YAP antibody (ab52771) and recovered by adding protein G magnetic beads at 4°C for 2 hours (Invitrogen).

For LC/MS-MS, beads prepared from HT29-YAPdc nuclear extracts were washed with TEGN 150 buffer (20 mmol/L Tris, pH 7.65, 150 mmol/L NaCl, 3 mmol/L $MgCl_2$, 0.1 mmol/L EDTA, 10% glycerol, and 0.01% NP40) and 5 times with 20 mmol/L ammonium bicarbonate at 56°C for 30 minutes. Disulfide bridges were then reduced by incubation by 10 mmol/L DTT in ammonium bicarbonate. Cysteine residues were alkylated by incubation with 15 mmol/L iodoacetamide in ammonium bicarbonate. Proteins on beads were digested with 40 ng/μL trypsin overnight (Promega Sequencing Grade Modified Trypsin). After stopping the reaction with 5% trifluoroacetic acid, beads were washed with ammonium bicarbonate, desalted, and concentrated with Ziptip C18.

Published OnlineFirst January 20, 2021; DOI: 10.1158/1541-7786.MCR-20-0462

Peptides were analyzed by LC/MS-MS using a nanoacquity UPLC (Waters) coupled with a Q-Exactive Orbitrap MS instrument (Thermo Scientific). Peptides were separated by online C18 reversed phase (analytical column: nanoAcquity BEH C18, 1.7 μm, 75 μm × 250 mm). A 2h -linear gradient of acetonitrile in 0.1% formic acid (5%–35%) was used. MS analysis was done in data-dependent mode (top ten) with the following parameters: for MS, a resolution of 70,000 FWHM, an automatic gain control (AGC) of 3e6 ions, and a maximum injection time of 120 ms. For MS/MS, an m/z mass range between 200 and 2,000, an AGC of 5e4 ions, a maximum injection time of 60 ms, and a resolution of 17,500 FWHM. MS data were analyzed with MaxQuant version 1.6.5.0 software (https://www.maxquant.net/maxquant/, RRID: SCR_014485). Protein identification was based on at least two peptides and one unique peptide per protein using the human proteome from the Uniprot database (release June 2019, 20,416 sequences). Trypsin was used as specific enzyme with two possible missed cleavages. Carbamidomethylation of cysteine residues was set as fixed modification, and N-terminal acetylation and methionine oxidation were selected as variable modifications. The FDR was set to 1% for all Peptide Spectrum Matches and protein levels, followed by relative label-free quantification. The analysis of the proteins identified in each sample was completed with the Perseus software (https://www.maxquant.net/perseus/), and proteins were annotated using gene ontology terms relative to cellular components.

Chromatin immunoprecipitation and re-chromatin immunoprecipitation experiments and PCR

Protein cross-linking to DNA was performed at room temperature by adding drop-wise formaldehyde to the culture medium for 10 minutes (1%, final concentration). Chromatin was prepared from YAPdc-HT29 and -RKO nuclear samples after two successive extraction steps at 4°C for 10 minutes, as previously described (19). Briefly, nuclei were resuspended in 50 mmol/L Tris (pH 8.0) containing 0.1% SDS, 1% NP-40, 0.1% Na-deoxycholate, 10 mmol/L EDTA, 150 mmol/L NaCl, and protease inhibitors cocktail (Roche, 04693124001) and were sonicated with a Bioruptor Power-up device (Diagenode) to obtain genomic DNA fragments with a bulk size of 150 to 300 bp. Chromatin was recovered by centrifugation at 14,000 × *g* and 4°C for 10 minutes. Immunoprecipitation (IP) was carried out by incubation (4°C for 2 hours) with specific antibodies directed against YAP, RARα, RARγ, and RXRα and the corresponding nonspecific IgGs as control. Immune complexes were recovered by adding protein G magnetic beads at 4°C (overnight) followed by extensive washes. Immune complexes were eluted at 65°C in Tris-EDTA buffer supplemented with 1% SDS. Formaldehyde cross-linking was then reversed at 65°C overnight by adding 0.2 mol/L NaCl (final concentration).

DNA was extracted using the NucleoSpin Gel and PCR Clean-up Kit (Macherey-Nagel). QPCR was performed using SsoFast EvaGreen Supermix 2× (Bio-Rad). For estimation of chromatin enrichment, chromatin immunoprecipitation (ChIP)-qPCR data are represented as percentage of IP/input signal. For re-ChIP experiments, the eluted immune complexes were subjected to another IP step (IP-RXRα), according to the protocol described above. Antibodies and primer sequences are listed in Supplementary Table S1.

Statistical analyses

Results are expressed as the mean ± SD of at least three separate experiments. Statistical significance was assessed with the Student *t* test.

Results

YAP activation upregulates *RAR* and *CYP26A1* transcripts

We first examined whether constitutive YAPdc activation modulates RAR expression in colorectal cancer cells HT29 and 5F31 after stable ectopic expression of the proteasome-resistant, FLAG-tagged YAP(S127A) mutant. The Ser/Ala substitution at position 127 in YAPdc sequence prevents YAP phosphorylation by the Hippo pathway and promotes oncogenic YAP nuclear localization and transcriptional activities (20).

Quantitative qRT-PCR analysis revealed the strong upregulation of RARα ($P < 0.001$) and RARγ transcripts ($P < 0.01$) in YAPdc-HT29 and -5F31 cells compared with corresponding control vector cells (**Fig. 1A**). Western blot (WB) analysis indicated that also RARγ protein levels were increased ($P < 0.05$) following ectopic expression of YAPdc protein (lower band vs. wt-YAP, upper band) in both HT29 and 5F31 cells (**Fig. 1B**). WB of RARγ in nuclear/cytoplasmic fractions prepared from HT29 cells and IF analysis determined that YAP-induced RARγ expression occurred in the nucleus (**Fig. 1C** and **D**), whereas RARα expressed at the cell membrane and cytoplasm, although it was also present in the nucleus (**Fig. 1D**). Then we examined whether YAP activation affected RAR transcriptional activity by quantifying *CYP26A1* expression, an RAR target gene that contains several RARE motifs in its promoter (21). In YAPdc-HT29 and -5F31 cells, *CYP26A1* transcript levels were increased by 5- to 6-fold compared with control cells ($P < 0.001$ and $P < 0.01$, respectively; **Fig. 1E**). To confirm YAP implication in RARα and RARγ expression, we knocked down YAP expression by siRNA. YAP silencing decreased RARγ levels in both HT-29 and 5F31 cells as shown in a representative WB from three experiments (**Fig. 1F**). Moreover, RARα and RARγ transcript levels were consistently reduced by 40% to 60% in YAP-silenced HT29 and 5F31 cells compared with control (**Fig. 1G**; $P < 0.01$ and $P < 0.05$ in HT29 cells; and $P < 0.001$ for both RARα/γ in 5F31 cells). Similarly, *CYP26A1* transcripts were decreased by 45% and 52% in YAP-silenced HT29 and 5F31 cells (**Fig. 1H**; $P < 0.001$ and $P < 0.01$). Our data indicate that YAPdc upregulates RARα/γ expression and transcriptional activity.

5-FU resistance and YAP activation reinforce colorectal cancer cell stemness traits

We previously showed that a small fraction of HT29 cells express several membrane-associated stem cell–like markers, i.e., CD24, CD44, CD133, and CXC motif chemokine receptor type 4 (16, 22). Conversely, most (90%) 5-FU–resistant 5F31 cells express at least one stemness marker, suggesting that they display stem cell–like features. Accordingly, we observed that the transcript levels of *ALDH1A3* and *LGR5* were 4-fold higher in 5-FU–resistant 5F31 than in 5-FU–sensitive HT29 cells (**Fig. 2A**, $P < 0.01$). These findings support the general hypothesis that in colorectal cancer cells, resistance to 5-FU–based chemotherapy relies at least in part on the expression of stemness traits and regulators. We then observed that compared with control cells, YAPdc in HT29 and 5F31 cells produced additional accumulation of transcript levels from the RARE-regulated genes *ALDH1A3* (6.7- and 4.3-fold, $P < 0.001$), *LGR5* (2.3- and 2.1-fold $P < 0.001$), and *OCT4* (2.3- and 1.9-fold, $P < 0.05$ and $P < 0.001$; **Fig. 2B**). Consistently, immunoblot analysis revealed that YAP activation increased ALDH1A3 accumulation in these two models (**Fig. 2D**). IF analysis confirmed the increased ALDH1A3 and OCT4 expression in YAPdc-expressing cells (**Fig. 2C**), as well as of LGR5, which was scarcely detectable in control cells. In contrast, YAP silencing in HT29 and 5F31 cells resulted in downregulation of

Published OnlineFirst January 20, 2021; DOI: 10.1158/1541-7786.MCR-20-0462

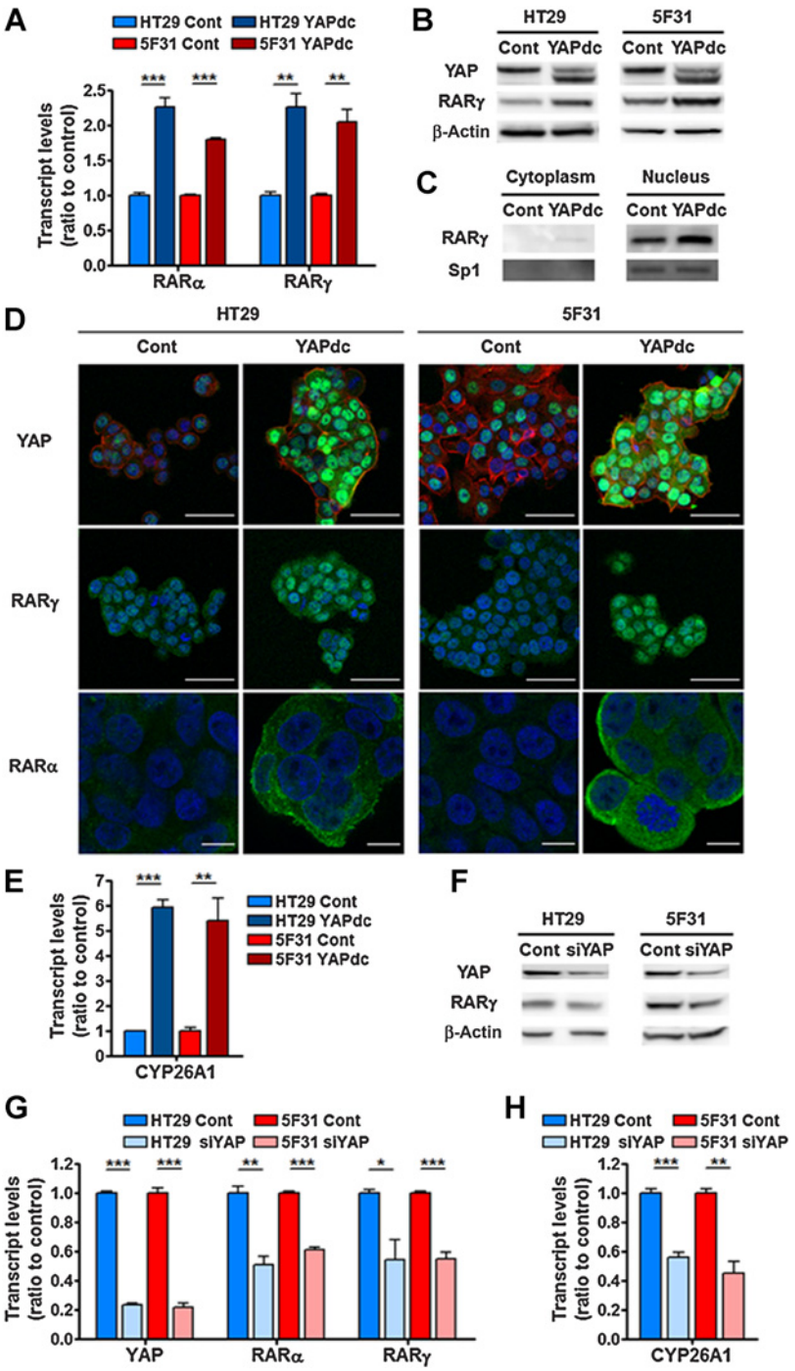

Figure 1.

YAP pathway activation upregulates RARα and RARγ in 5-FU–sensitive HT29 cells and their 5-FU–resistant 5F31 counterparts. **A,** Transcript levels of RARα and RARγ quantified by qRT-PCR in control empty vector (Cont)– and YAPdc-transfected HT29 and 5F31 cells. **B,** WB analysis of YAP and RARγ expression in control, YAPdc-transduced HT-29 and 5F31 cells. **C,** RARγ immunoblotting in cytoplasmic and nuclear extracts. Sp1 was used as nuclear marker in HT29 cells. **D,** Subcellular distribution of YAP, RARγ, and RARα by IF (green labeling). Nuclei were stained with DAPI. For YAP analysis (in top plots), F-actin was labeled with rhodamine phalloidin (red). Scale bars, 50 μm (YAP, RARγ) and 10 μm (RARα). **E,** *CYP26A1* transcript quantification by qRT-PCR. **F,** Effect of YAP siRNA on YAP and RARγ protein levels. **G** and **H,** *YAP, RARα, RARγ*, and *CYP26A1* transcript levels in control vector (Cont) and YAPdc-HT29 and -5F31 cells. Data are the mean ± SD of at least three separate experiments. Statistical significance was assessed with the Student *t* test. *, $P < 0.05$; **, $P < 0.01$; $P < 0.001$; ***, $P < 0.001$.

transcript levels encoding ALDH1A3 (63%–55%, $P < 0.001$ and $P < 0.01$), LGR5 (27%–29%, $P < 0.01$ and $P < 0.05$), and OCT4 (58%–53%, $P < 0.01$), as compared with control cells (**Fig. 2E**). Consistently, YAP knockdown decreased the self-renewal capacity of HT29 and 5F31 intestinal epithelial spheroids by 32% and 39%, respectively ($P < 0.05$, **Fig. 2F**).

RARs mediate YAP-induced stem cell–like phenotypes

Given that YAPdc ectopic expression in HT29 and 5F31 cells led to upregulation of RARs and RARE-regulated stemness genes and promoted self-renewal, we determined whether RAR-RXR signaling pathways were implicated in YAP-mediated cancer cell stemness. As shown in **Fig. 3A**, pharmacologic blockade of the RAR pathway by BMS 493 (a pan-RAR inverse agonist of RAR/RXR heterodimers) reduced *ALDH1A3* and *LGR5* transcript levels in YAPdc-HT29 cells (2.2-fold for both) and YAPdc-5F31 cells (2.8- and 2-fold, respectively), versus HT29 and 5F31 control cells. Next, we quantified the self-renewal capacity of HT29 and 5F31 cells incubated with BMS 493 for 24 hours and then cultured in BMS 493–free medium for 15 days. Representative images of sphere

Published OnlineFirst January 20, 2021; DOI: 10.1158/1541-7786.MCR-20-0462

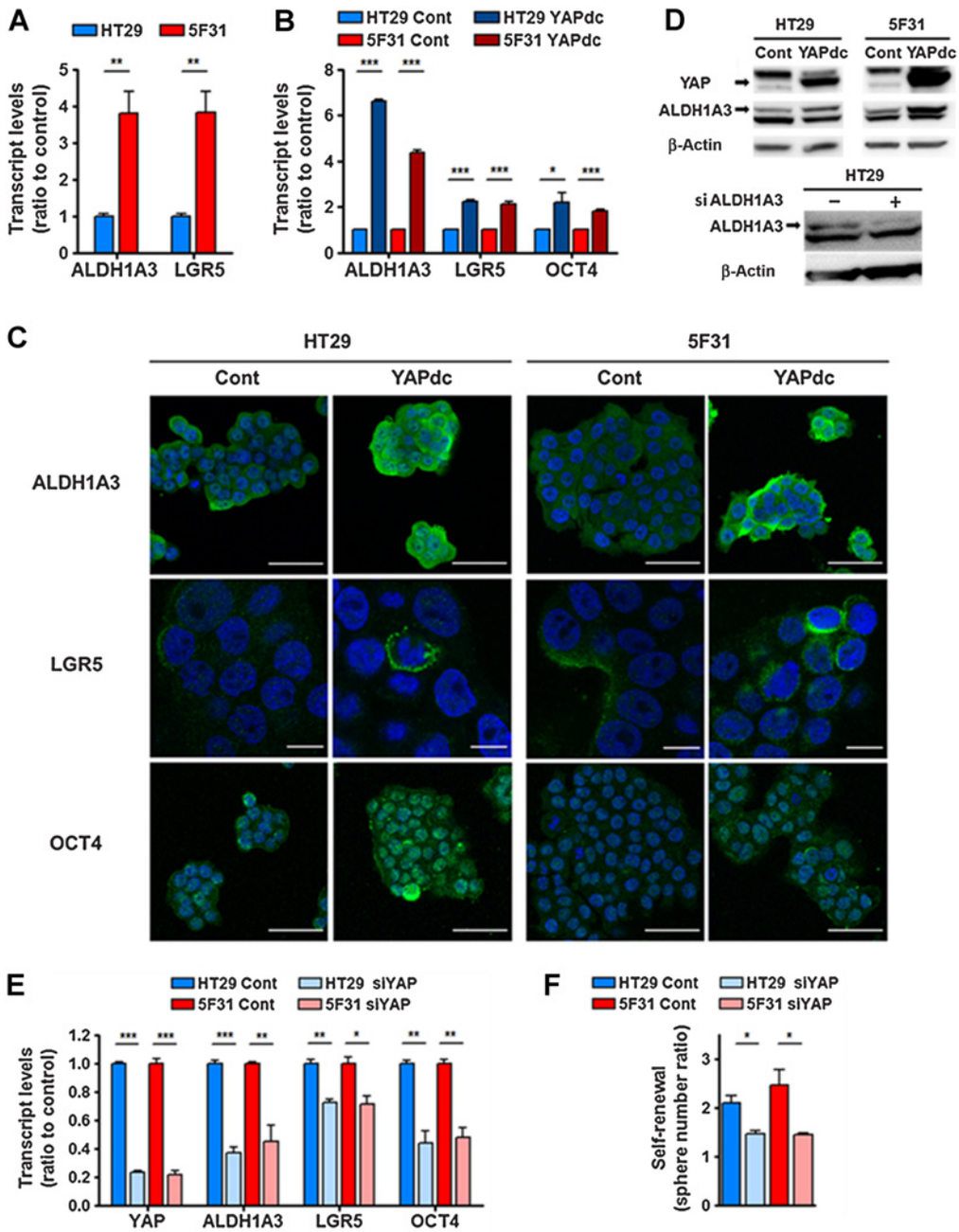

Figure 2.

YAP pathway activation upregulates stemness markers and promotes self-renewal in HT29 and 5F31 cells. **A,** *ALDH1A3* and *LGR5* transcripts' quantification by qRT-PCR in parental HT29 cells (blue bars) and 5-FU–resistant 5F31 cells (red bars). **B,** Effect of YAPdc on transcript levels encoding the stemness markers ALDH1A3, LGR5, and OCT4. **C,** IF analysis of ALDH1A3, LGR5, and OCT4 in YAPdc- and control vector–transfected HT29 and 5F31 cells (scale bars, 50 and 10 μm). **D,** WB analysis of YAP and ALDH1A3 in control (empty vector)- and YAPdc-transfected HT29 and 5F31 cells. β-Actin was used as loading control. ALDH1A3 knockdown by siRNA allowed us to determine the identity of ALDH1A3 protein as the upper WB band. **E,** Effects of YAP silencing by siRNA (siYAP) on *YAP, ALDH1A3, LGR5*, and *OCT4* transcript levels. Control cells are transfected with control si-RNA. **F,** Self-renewal capacity of control- and YAP-silenced HT29 and 5F31 cells (siYAP) assessed by counting sphere-forming units. Data are the mean ± SD of at least three separate experiments. Statistical significance was assessed with the Student *t* test. *, $P < 0.05$; **, $P < 0.01$; ***, $P < 0.001$.

assays in HT29 and 5F31 cells are illustrated in **Fig. 3C** (inserts). A major decrease (72% and 77%, $P < 0.001$) in sphere-forming unit generation after passaging was observed in the presence of BMS 493, as compared with untreated cells (**Fig. 3B**). Then, to determine the implication of vitamin A and RA metabolism in self-renewal, we cultured HT29 and 5F31 epithelial spheroids in vitamin A–free medium (Vit.A-free). In the absence of vitamin A, self-renewal was significantly reduced by 34% in HT29 spheroids and by 46% in 5F31

Published OnlineFirst January 20, 2021; DOI: 10.1158/1541-7786.MCR-20-0462

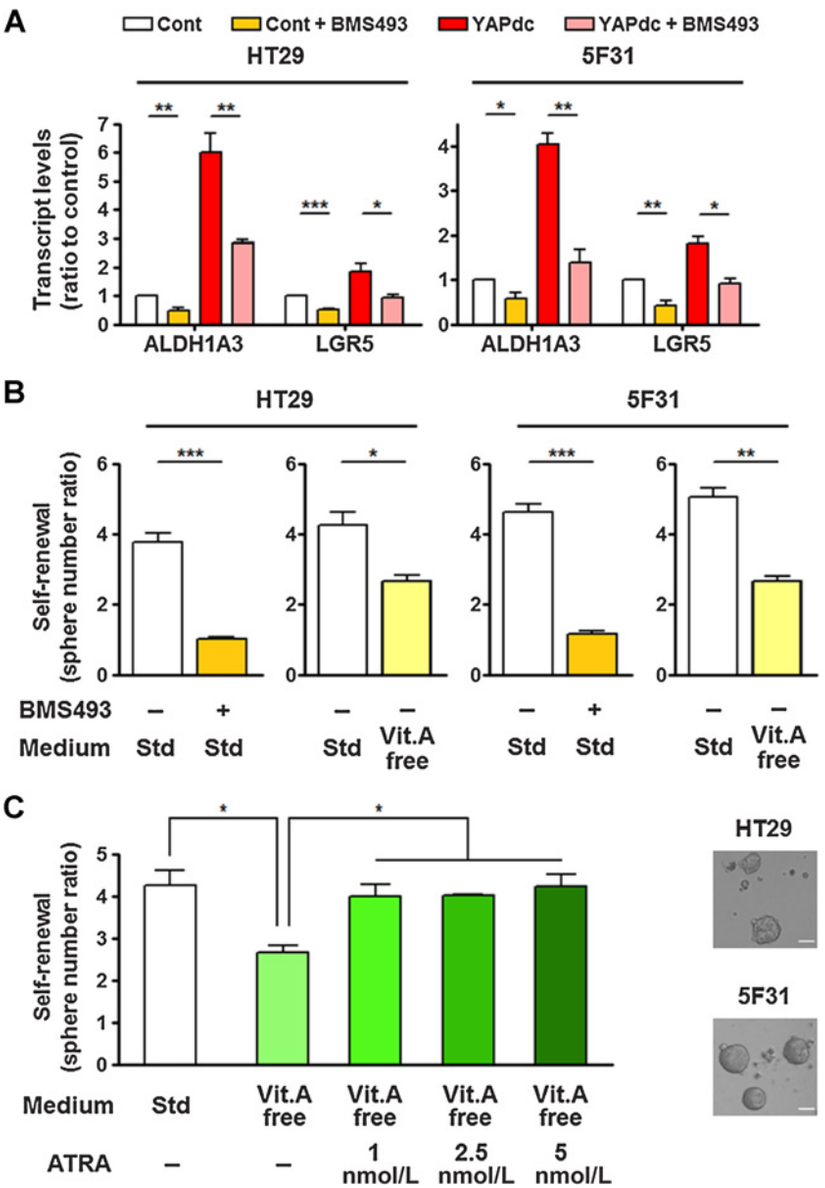

Figure 3.

Consequences of RAR pathway blockade by BMS 493, vitamin A depletion, and ATRA on *ALDH1A3* and *LGR5* transcript levels and self-renewal capacity. **A,** Effect of the pan-RAR inverse agonist BMS493 on *ALDH1A3* and *LGR5* transcript levels in control (empty vector) and YAPdc-HT29 and -5F31 cells. **B,** Effect of BMS493 and vitamin A removal (Vit.A free) on self-renewal of HT29 and 5F3 spheroids. **C,** Effect of ATRA (1–5 nmol/L) on self-renewal, i.e., formation of HT29 sphere-forming units cultured in the presence and absence of vitamin A, as indicated. Inserts, Representative images of control HT29 and 5F31 spheroids. Data are the mean ± SD of at least three separate experiments. Statistical significance was assessed with the Student *t* test. *, $P < 0.05$; **, $P < 0.01$; ***, $P < 0.001$.

spheroids (**Fig. 3B**; $P < 0.05$ and $P < 0.01$, respectively). Most interestingly, the inhibitory effect of vitamin A removal on HT29 self-renewal was abrogated by addition of very low ATRA concentrations (1–5 nmol/L) that are within the plasma concentration range (about 2 nmol/L) observed in healthy humans (ref. 23; **Fig. 3C**).

Identification of YAP-binding partners

Given our data in **Fig. 1A–C** showing that nuclear YAP activation resulted in nuclear RARγ overexpression at transcript and protein levels, we hypothesized that YAPdc could induce the formation of a nuclear YAP–RARγ complex in colorectal cancer cells. By using the proximity ligation assay in HT29-YAPdc cells, we revealed the nuclear/perinuclear colocalization and interaction of YAP with RARγ (**Fig. 4A**). Accordingly, we identified RARγ and RXRα as YAP-interacting partners in YAP immunoprecipitates (YAP-IP) and subsequent WB with antibodies against RARγ and RXRα in HT29-YAPdc cells (Supplementary Fig. S1).

In line with these findings, we anticipated that the YAP–RARγ heterodimeric complex might be involved, at least in part, in the regulation of the YAP/RAR-RXR cross-talk in the present study. According to our starting hypothesis, a systematic analysis of YAP-binding partners with special reference to RAR-RXR signaling elements was undertaken in HT29-YAPdc nuclear extracts following YAP-IP and proteomic analysis. We identified a set of 115 proteins binding selectively YAP (**Fig. 4B**; Supplementary Table S2). This set of 115 YAP-interacting proteins included a series of 82 proteins linked with an etiologic association with the nucleus. Mass spectrometry analysis identified known signaling elements that specifically interact with YAP in the canonical Hippo–YAP pathway: namely STK3/MST2 that induces YAP phosphorylation/cytoplasmic sequestration; the cytoplasmic/nuclear scaffold AMOT (Angiomotin)-dependent YAP-Merlin (NF2) complex and its downstream YAP targets, the TEAD1,3,4 nuclear transcription factors (**Table 1**). Most importantly, we uncovered that RXRα/β and γ physically interact with

Published OnlineFirst January 20, 2021; DOI: 10.1158/1541-7786.MCR-20-0462

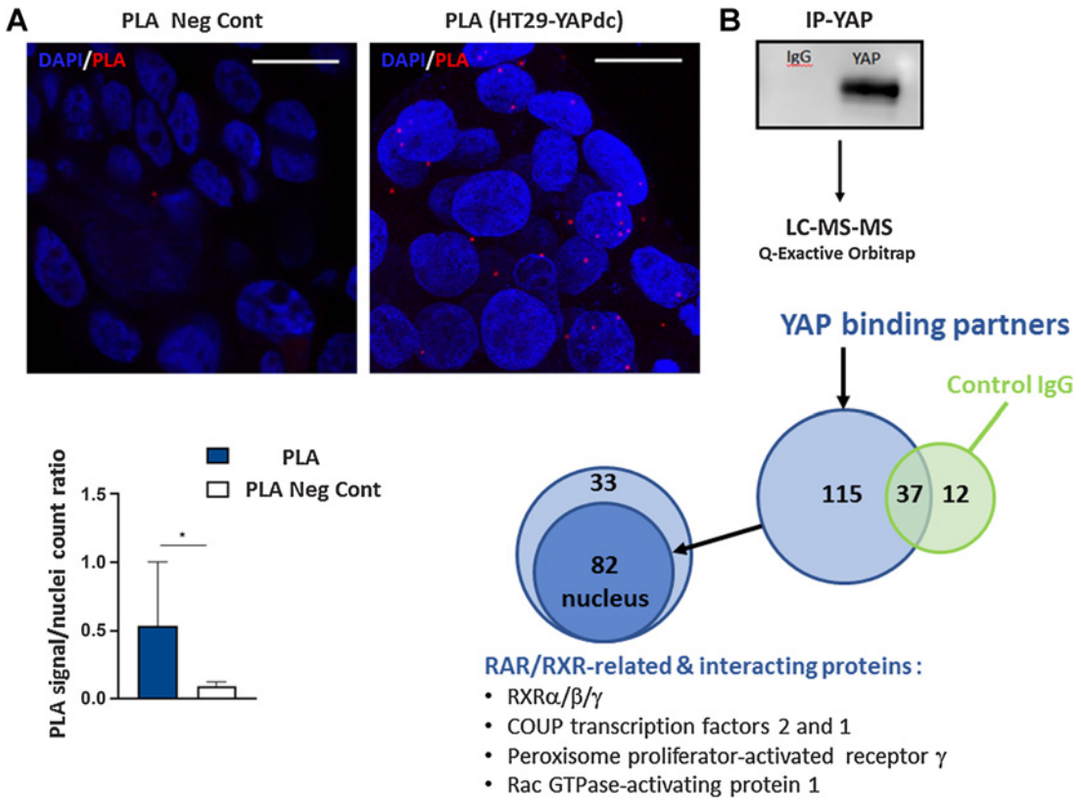

Figure 4.

Proximity-dependent labeling and identification of YAP-binding proteins. **A,** Proximity ligation assay was performed in YAPdc-HT29 cells (right), using the primary anti-YAP and -RARγ antibodies. Compared with the negative control (on the left; i.e., absence of the corresponding primary antibodies against YAP and RARγ), we determined the proximity ligation assay signal in ten fields by confocal microscopy imaging using maximum intensity projection of z-stack images, according to the Duolink protocol. Then, we quantified the results as the ratio of the proximity ligation assay signal (i.e., number of intersection points) relative to the total number of nuclei (three separate experiments, $P < 0.05$). Nuclei were labeled with DAPI and YAP–RARγ complex in red. Scale bar, 10 μm. **B,** Mass spectrometry–based proteomics analysis of YAP-binding partners in YAP-IP and YAP WB was done in nuclear extracts prepared from HT29-YAPdc cells. Venn diagrams show the overlapping between proteins identified in YAP-IP versus control IgG. Among the 115 proteins identified by IP-YAP, 82 were associated with the nucleus.

YAP1. We also identified a series of YAP-interacting candidates implicated in essential transcriptional mechanisms and RAR signaling pathways, namely orphan nuclear COUP-TF1/TF2 transcription factors (*NRF1/F2*); PPARγ (encoded by *PPARG* and part of the PPARG–RARα complex); the Rac-GTPase–activating protein (encoded by *RACGAP1*); and the N^+/K^+ exchange regulatory cofactor NHE-RF2 (*SLC9A3R2*) that regulates YAP activation and cytoplasmic sequestration (Hippo-like pathway), respectively. Complementary to our proteomic study, other potential YAP-binding proteins are listed and classified in Supplementary Tables S2 and S3 (parts A and B), according to several biological and functional criteria related to the present study.

Binding of YAP/RAR-RXR interactome at RAREs in stemness genes

Analyses of the 5′ flanking regions of the *ALDH1A3* and *LGR5* promoters in the Eukaryotic Promoter Database revealed the presence of several RAREs (5′-GGGTCATCGCCCTGCCA-3′) and TEADs (G(A)GA(T/C)ATG) according to their respective consensus sequences (**Fig. 5A**). Therefore, we carried out ChIP experiments to determine whether YAP and RARs interact at the RARE promoter fragments present at positions -244 -61 (*ALDH1A3*) and -825 -727 (*LGR5*). We provide evidence for co-occupancy of YAP, RARα, RARγ, and RXRα at these genomic regions containing regulatory RAREs (**Fig. 5B**). ChIP and re-ChIP experiments with RXRα antibody bring to light the formation of a YAP–RXRα molecular complex at the *ALDH1A3* and *LGR5* promoters (**Fig. 5C**). YAP and RXR-RAR binding occurred at promoter regions devoid of potential TEAD-binding sites (**Fig. 5A**). In contrast, no enrichment in RXRα was observed on irrelevant regulatory sequences of the P*AX6* promoter (primers are listed in Supplementary Table S1) after successive YAP-ChIP and RXRα–re-ChIP experiments (0.9 for RXRα vs. 1 for IgG). Similarly, in control HT29 cells transfected with the pLPCX empty retroviral vector, the chromatin enrichment in YAP, RXRα, RARα, and RARγ at the *ALDH1A3* and *LGR5* proximal RAREs was either barely detectable or detected at a much lower intensity in comparison with HT29-YAPdc cells (**Fig. 5**; Supplementary Fig. S2, $n = 2$ experiments).

Taken together, our data support our initial hypothesis that the YAP/RAR-RXR cross-talk promoted by oncogenic nuclear YAP upregulates stemness characteristics in both 5-FU–sensitive and –resistant colorectal cancer cells, providing the initial proof of concept of the study (**Fig. 6**). Validation of these signaling and transcriptional pathways was performed in epithelial RKO cells, another parental

Published OnlineFirst January 20, 2021; DOI: 10.1158/1541-7786.MCR-20-0462

Table 1. Proteomics of YAP-binding partners according to YAP/RAR-RXR cross-talk.

Relationship with the YAP-RAR/RXR cross-talk	
Transcriptional enhancer factors TEF-1, TEF-5, and TEF-3	***TEAD1, 3, 4*** Transcription factors involved in Hippo, Wnt, TGFβ, and EGFR oncogenic pathways
Angiomotin-like protein 2	***AMOTL2*** YAP–TEAD–Merlin complex
Merlin	***NF2*** ERM family, inhibits Ras/Rac activity, interacts with LATS, YAP1 dephosphorylation, and nuclear shuttling
Serine/threonine-protein kinase 3	***STK3/MST2*** YAP Phosphorylation in Hippo pathway and nuclear LC3 (autophagy)
RXRα/β/γ	***RXRα/β/γ*** NRs, RXR–RXR homodimers Permissive heterodimers RXR-(PPAR, LXR, FXR, PXR, CAR) Nonpermissive heterodimers RXR-(VDR, TR, and RAR)
COUP transcription factor 2, and 1	***NR2F2 and F1*** NR, Transcription steroid–thyroid receptors family, RXR sequestration, NR2F2-RXR heterodimers, 9-*cis*-retinoic acid, tumor angiogenesis, EMT, oncogene/suppressor balance
Peroxisome proliferator-activated receptor gamma	***PPARG*** NR, PPARG–RARα complex
Rac GTPase-activating protein 1	***RACGAP1*** Overexpressed in nuclei of CRC cells Poor prognosis in CRC. Oncogenic, metastasis. Nuclear YAP activation in HCC
Na^+/K^+ exchange regulatory cofactor NHE-RF2	***SLC9A3R2*** Component of the dystrophin glycoprotein Complex DGC involved in YAP sequestration (Hippo-like). Cytoskeleton–ECM connections

Abbreviations: CRC, colorectal cancer; ECM, extracellular matrix; EMT, epithelial–mesenchymal transition.

colorectal cancer cell line stably transfected with the constitutively activated YAP(S127A) mutant. In this model, oncogenic YAPdc leads to increased transcripts levels implicated in the YAP/RAR-RXR interplay, namely *RARγ*, the RARE-regulated *OCT4* and *ALDH1A3* stemness genes, without significant effect on *SOX2* transcripts (Supplementary Fig. S3A). Ectopic expression of YAPdc in RKO cells is shown in comparison with control pLPCX empty vector–transfected RKO cells. Furthermore, genomic co-occupancy of RXRα at the proximal RARE region (- 244, -61) of the *ALDH1A3* gene was demonstrated by ChIP/qPCR in RKO-YAPdc cells (Supplementary Fig. S3B) as well as co-occupancy of YAP, RARα, and RARγ at lower levels.

Finally, we have identified RXRα as the major retinoid X receptor subtype interacting with the proximal regions of the RARE promoters of stemness genes in YAPdc-HT29 cells (*ALDH1A3* and *LGR5*), RKO (*ALDH1A3*), and to a lesser extent in control HT29 empty vector cells (Fig. 5B and C; Supplementary Figs. S2 and S3). In addition, we revealed the presence of another molecular complex between RXRα and YAP at these RARE sequences in HT29-YAPdc cells (**Fig. 5C**). Altogether, our data underline the critical contribution of RXRα and RARα/γ in the activation by YAP of proximal RAREs in these two stemness genes. Consistently, our proteomic study in **Table 1** reveals RXRα/β/γ as YAP-binding partners.

Discussion

Our data together uncover a new signaling YAP/RAR-RXR cross-talk related to the activation status of the transcriptional coactivator YAP in 5-FU–sensitive and –resistant colorectal cancer cells. We anticipate that deficiencies in Hippo tumor-suppressor pathway components by loss-of-function mutations associated with oncogenic YAP hyperactivation in human cancers and other diseases take part in the processing of the YAP/RAR-RXR cross-talk and establishment of alternative mechanisms regulating stemness maintenance. At the genomic level, we revealed the co-occupancy of YAP and RARs at RAREs in promoter sites of the *ALDH1A3* and *LGR5* stemness genes. Persistence of the dynamic YAP/RAR-RXR cross-talk in 5-FU–resistant colorectal cancer cells provides promising clues for developing effective therapies to target the YAP/RAR-RXR cross-talk induced by oncogenic YAP and Hippo deficiencies in both 5-FU–sensitive and 5-FU–resistant colorectal cancer.

In the present study, parental HT29 cells and their 5-FU–resistant 5F31 counterparts were investigated under a gradient of YAP activation. At a first level of ectopic YAPdc expression, we observed coordinated and coherent increases in RARα/γ transcripts and proteins associated with YAP and RARγ nuclear accumulation, induction of the RARE target genes *CYP26A1, ALDH1A3*, and *LGR5*, and upregulation of the stemness gene *OCT4* known to positively control the level of RARγ (24). These signaling responses reinforce stemness traits and self-renewal competence of HT29 and 5-FU–resistant 5F31 cells. Of note, 5-FU–resistant 5F31 cells were previously demonstrated to be particularly endowed by cancer stem cell markers and self-renewal potential (16). At the second level, endogenous YAP knockdown by siRNAi led to inverse downregulation of RARα/γ, the RA target gene *CYP26A1*, and stemness markers/regulators (ALDH1A3, LGR5, and OCT4). These convergent data extend our previous studies on the implication of YAP activation in the spheroid-forming potential and reversible quiescence linked to 5-FU resistance in stem cell–like colorectal cancer cells (16, 17).

Dual roles of the YAP–RARγ complex at cytoplasmic and nuclear levels

RARγ signaling has a central role in chromatin remodeling, transcriptional activation, hematopoietic stem cells (HSC) maintenance, and self-renewal/differentiation balance in embryonic stem cells (25). In contrast, RARα is mainly involved in HSC differentiation. In bone marrow of $RAR\gamma^{-/-}$ mice, but not of $RAR\alpha^{-/-}$ mice, HSC number is reduced, whereas the number of more mature progenitors is increased (26). In our study, the YAP/RAR-RXR signaling cross-talk in HT29-YAPdc cells is supported by a series of genetic, cellular, and molecular clues related to identification of a YAP–RARγ complex by proximity ligation assay and YAP pulldown assays (**Fig. 4A**; Supplementary Fig. S1) and the upregulation of RARE-inducible genes *CYP26A1, ALDH1A3*, and *LGR5*. Hence, this signaling and transcriptional YAP/RAR-RXR cross-talk is likely to be promoted and fueled by YAP-induced upregulation of RAR-RXR transcriptional elements, including induction of RARγ and the *OCT4* stemness transcription factor gene involved in RARγ expression (24). In addition, our proteomic analysis indicated that both Merlin and AMOT (i.e., angiomotin) are YAP nuclear interactors comprising TEADs 1, 3, and 4. This finding is in agreement with the canonical cytoplasmic/nuclear YAP shuttling observed in Hippo-deficient cancer cells via induction of multiple genomic activities. Indeed, AMOT functions as a scaffolding protein that enables the translocation of the cytoplasmic AMOT/YAP/Merlin complex to the nucleus mediated by AMOT

Published OnlineFirst January 20, 2021; DOI: 10.1158/1541-7786.MCR-20-0462

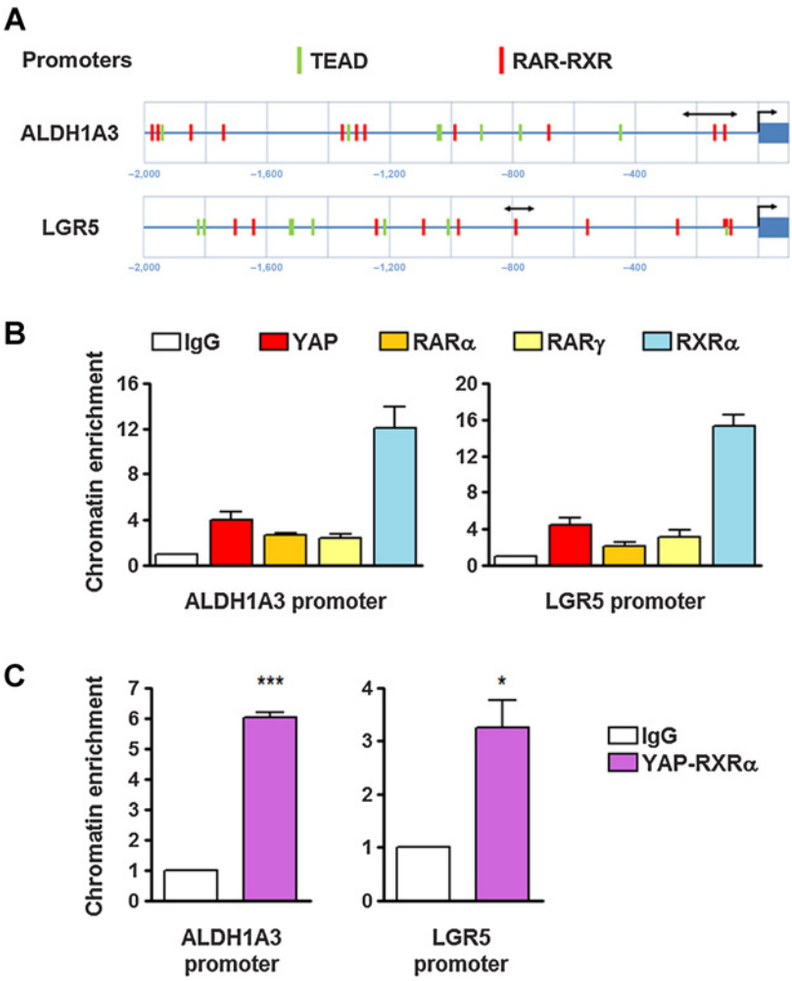

Figure 5.

ALDH1A3 and *LGR5* promoter sequences implicated in YAP, RARα/γ, and RXRα molecular interactions in HT29-YAPdc cells. **A,** Schematic diagram of *ALDH1A3* and *LGR5* proximal promoters showing consensus RAREs (red vertical bars) and TEADs binding sites (green vertical bars) and the regions analyzed by ChIP assays (double arrows). **B,** Promoter sequence co-occupancy by YAP, RXRα, and RARα/RARγ was identified by YAP-induced ChIP in HT29-YAPdc nuclear extracts, using the corresponding specific antibodies. **C,** Re-ChIP by successive IP-YAP and IP-RXRα revealed *ALDH1A3* and *LGR5* promoter sequences co-occupancy by the YAP–RXRα complex, using the same specific antibodies. Data are mean ± SD from five separate experiments.

hypophosphorylation at serine 176 (27, 28). This trimeric complex facilitates nuclear YAP/TEAD interaction and activation of the promoters and distal enhancer regions of canonical YAP-TEAD target genes (29, 30). Therefore, it is tempting to consider that the TEAD-AMOT/YAP/Merlin assembly in our study participates with the YAP–RARγ complex in nuclear targeting of the transcriptional coactivator YAP to activate canonical YAP-TEAD pathways, together with the newly identified YAP–RAR/RXR-dependent cross-talk. Thus, in case of Hippo deficiencies observed in cancers, it is likely that both the nuclear TEAD–AMOT–YAP–Merlin and alternative YAP/RAR-RXR pathways are operational by targeting respectively TEAD and RARE elements in ALDH1A3 and LGR5 promoters, in our study. These data identified the cytoplasmic YAP–RARγ complex as a new integral regulatory element of the authentic tumor-suppressive functions of the Hippo signaling kinases cascade in SW480 human colorectal cancer cells (31). In this context, our data shed light on the opposing roles of the YAP–RARγ complex that acts as Hippo activator/YAP inhibitor in the cytoplasm (31) while promoting colorectal cancer cell stemness maintenance, 5-FU-chemoresistance, and nuclear activation of RAR/RXR and RARE-dependent stemness genes.

YAP as a transcriptional RAR-RXR coactivator

Accumulating evidence supports the paramount importance of YAP binding to DNA-remodeling proteins for regulating chromatin structure, dynamics, and accessibility of transcription factors to promoter and enhancer elements involved in the transcriptional machinery, including elongation events (32). In agreement with YAP coactivator pleiotropic mechanistic roles on the transcriptional regulation of target genes with oncogenic or tumor-suppressive functions, ChIP and re-ChIP analyses of YAP in HT29-YAPdc cells bear the notion that this cofactor is engaged in a new genomic interactome that includes RARα/γ and RXRα transcription factors. This molecular interactome will likely be fueled by YAP-induced RARα/γ overexpression and YAP–RXRα molecular interactions, leading to occupation of the proximal RAREs in *ALDH1A3* and *LGR5* stemness genes and consequently to their upregulation (**Fig. 6**). According to our current YAP/RAR-RXR cross-talk hypothesis, blocking the YAP and RAR pathways by siRNAs or pharmacologic inhibitor restricted YAP-induced expression of stemness traits (stemness genes and self-renewal).

Collectively, our study will bring an important paradigm to nuclear YAP functionality engaged in a new transcriptional interplay, besides its classical DNA-binding partners, e.g., TEADs, CREB, SMADs, and the tumor suppressors Runx2 and p73. Thus, we can consider YAP as a novel transcriptional coactivator that targets colorectal cancer stemness maintenance through a genomic interactome at proximal RAREs of stemness genes. Another emphasis in our data was placed on the positive feedback regulation exerted by ATRA upstream signals converging to the transcriptional YAP/RAR-RXR platform. Indeed,

Published OnlineFirst January 20, 2021; DOI: 10.1158/1541-7786.MCR-20-0462

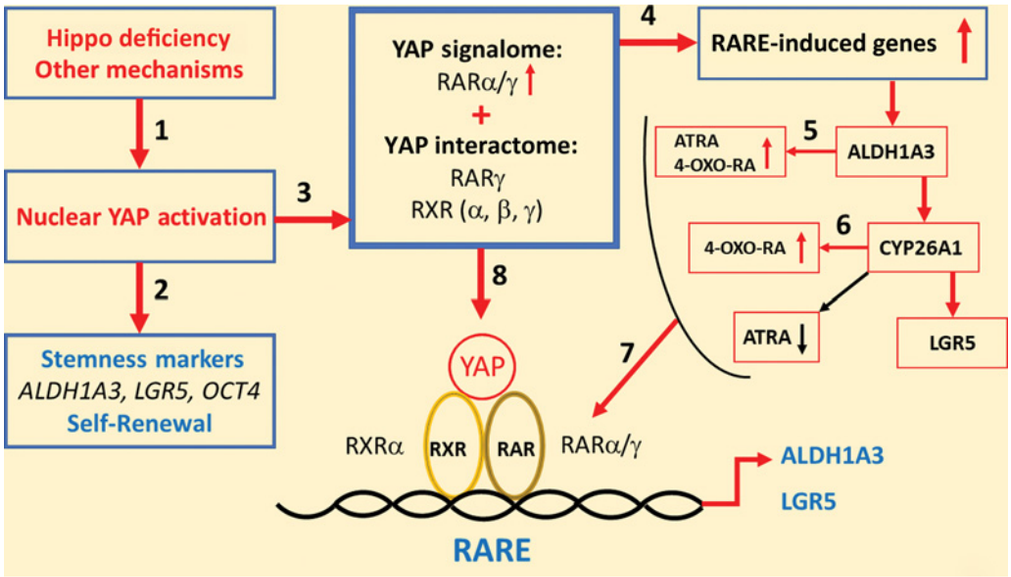

Figure 6.

Proposed model of YAP/RAR-RXR signaling cross-talk and genomic interactome. **1** and **2,** Global impact of nuclear YAP activation: Upregulation of stemness genes (*ALDH1A3, LGR5*, and *OCT4)* and self-renewal maintenance. **3,** Signalome of YAP-induced RARα/γ transcript/protein levels and molecular YAP/RAR-RXR interactomes visualized by proximity ligation assay, IP-YAP, and mass spectroscopy. **4,** Upregulation of the RARE-regulated genes *ALDH1A3, CYP26A1*, and *LGR5*. **5,** Generation by ALDH1A3 of the RAR ligands ATRA and 4-OXA-RA. **6,** Positive and negative regulation of 4-OXA-RA/ATRA balance by CYP26A1. **7,** Implication of RAR ligands in autocrine/intracrine activation loops regulating self-renewal maintenance: Partial inhibition by (**i**) BMS 493 (a pan-RAR inverse agonist of RAR/RXR heterodimers) and (**ii**) Vitamin A deficiency (rescued by 1 nmol/L ATRA). **7** and **8,** Signaling, molecular, and genomic convergences of the YAP/RAR-RXR cross-talk in self-renewal and RARE-induced transcription of stemness genes *ALDH1A3* and *LGR5*.

pharmacologic inhibition of ATRA-mediated RAR/RXR pathways and vitamin A deficiency weaken stemness traits and self-renewal. Of note, nanomolar ATRA concentrations rescued vitamin A deficiency in HT29 and 5F31 cells. Therefore, our data support the occurrence of dynamic links between YAP and RAR-RXR pathways that generate a constitutive regulatory self-activation loop through production of RAR ligands from ALDH1A3, vitamin A, and ATRA/retinoid metabolism (**Fig. 6**).

Selective elimination of subpopulations of stem cell–like cancer cells with acquired radiochemotherapy resistance, plasticity, and pluripotency will provide a beneficial therapeutic strategy to prevent tumor recurrence and metastasis in patients with 5-FU–responsive and –resistant cancer treated with 5-FU–based regimen. Inhibition of the canonical YAP/TAZ-TEAD activity is emerging as an attractive drug target in cancer therapy strategies in patients with cancer treated with 5-FU–based regimens. Clinically, the permissive roles of ATRA-mediated upstream YAP/RAR-RXR signals combined with nuclear YAP activation and *ALDH1A3* overexpression in our study may explain the limited impact of retinoid therapy in epithelial cancers. The stemness marker and effector ALDH1A3 is known to generate alternative stemness mechanisms initiated by ATRA synthesis from *all-trans* retinal oxidation to induce gene expression changes linked to differentiation and oncogenic responses (33, 34). Exclusion of noneligible patients with colorectal cancer with aberrant high YAP/TAZ and Ki-67 levels in residual metastases and shorter disease-free survival (16) can help improve the management of patients with colorectal cancer showing overexpression of the ATRA-forming enzyme ALDH1A3. Invalidation of the YAP/RAR-RXR cross-talk and ALDH1A3 pathways might represent complementary approaches to reverse resistances associated with 5-FU–based regimens in patients with aggressive and metastasized colorectal cancer.

Authors' Disclosures

No disclosures were reported.

Authors' Contributions

M. Bauzone: Data curation, formal analysis, methodology. **M. Souidi:** Data curation, formal analysis, methodology. **A.-F. Dessein:** Data curation, formal analysis, methodology, project administration. **M. Wisztorski:** Data curation, formal analysis, methodology. **A. Vincent:** Formal analysis, methodology, project administration. **J.-P. Gimeno:** Data curation, formal analysis, methodology. **D. Monté:** Formal analysis, methodology. **I. Van Seuningen:** Resources, project administration. **C. Gespach:** Conceptualization, formal analysis, validation, investigation, writing–original draft, project administration, writing–review and editing. **G. Huet:** Conceptualization, formal analysis, supervision, funding acquisition, validation, investigation, writing–original draft, project administration, writing–review and editing.

Acknowledgments

We thank Pr. I. Fournier (Clic-Imaging Platform, Lille University) for mass spectrometry and proteomics analyses and Marie Vandepeutte for IF analyses. This work was supported by Inserm, CNRS, grants from Fondation ARC, La Ligue Nationale Contre le Cancer (comité du Nord), SIRIC ONCOLille, Grant INCa-DGOS-Inserm 6041, and from "Contrat de Plan Etat Région" CPER Cancer 2007–2013. Marjolaine Bauzone received a predoctoral fellowship from the Ecole Doctorale Biologie-Santé.

The costs of publication of this article were defrayed in part by the payment of page charges. This article must therefore be hereby marked *advertisement* in accordance with 18 U.S.C. Section 1734 solely to indicate this fact.

Received May 19, 2020; revised November 10, 2020; accepted January 12, 2021; published first January 20, 2021.

References

1. Evans RM, Mangelsdorf DJ. Nuclear receptors, RXR, and the big bang. Cell 2014; 157:255–66.
2. Krezel W, Ruhl R, de Lera AR. Alternative retinoid X receptor (RXR) ligands. Mol Cell Endocrinol 2019;491:110436.
3. Gianni M, Ponzanelli I, Mologni L, Reichert U, Rambaldi A, Terao M, et al. Retinoid-dependent growth inhibition, differentiation and apoptosis in acute promyelocytic leukemia cells. Expression and activation of caspases. Cell Death Differ 2000;7:447–60.
4. Wang W, Yang J, Liu H, Lu D, Chen X, Zenonos Z, et al. Rapid and efficient reprogramming of somatic cells to induced pluripotent stem cells by retinoic acid receptor gamma and liver receptor homolog 1. Proc Natl Acad Sci U S A 2011; 108:18283–8.
5. De Angelis MT, Parrotta EI, Santamaria G, Cuda G. Short-term retinoic acid treatment sustains pluripotency and suppresses differentiation of human induced pluripotent stem cells. Cell Death Dis 2018;9:6.
6. Connolly RM, Nguyen NK, Sukumar S. Molecular pathways: current role and future directions of the retinoic acid pathway in cancer prevention and treatment. Clin Cancer Res 2013;19:1651–9.
7. Camargo FD, Gokhale S, Johnnidis JB, Fu D, Bell GW, Jaenisch R, et al. YAP1 increases organ size and expands undifferentiated progenitor cells. Curr Biol 2007;17:2054–60.
8. Cordenonsi M, Zanconato F, Azzolin L, Forcato M, Rosato A, Frasson C, et al. The Hippo transducer TAZ confers cancer stem cell-related traits on breast cancer cells. Cell 2011;147:759–72.
9. Barry ER, Morikawa T, Butler BL, Shrestha K, de la Rosa R, Yan KS, et al. Restriction of intestinal stem cell expansion and the regenerative response by YAP. Nature 2013;493:106–10.
10. Zheng Y, Pan D. The Hippo signaling pathway in development and disease. Dev Cell 2019;50:264–82.
11. Gumbiner BM, Kim NG. The Hippo-YAP signaling pathway and contact inhibition of growth. J Cell Sci 2014;127:709–17.
12. Gregorieff A, Liu Y, Inanlou MR, Khomchuk Y, Wrana JL. Yap-dependent reprogramming of Lgr5(+) stem cells drives intestinal regeneration and cancer. Nature 2015;526:715–8.
13. Barker N, van Es JH, Kuipers J, Kujala P, van den Born M, Cozijnsen M, et al. Identification of stem cells in small intestine and colon by marker gene Lgr5. Nature 2007;449:1003–7.
14. de Sousa e Melo F, Kurtova AV, Harnoss JM, Kljavin N, Hoeck JD, Hung J, et al. A distinct role for Lgr5(+) stem cells in primary and metastatic colon cancer. Nature 2017;543:676–80.
15. Shimokawa M, Ohta Y, Nishikori S, Matano M, Takano A, Fujii M, et al. Visualization and targeting of LGR5(+) human colon cancer stem cells. Nature 2017;545:187–92.
16. Touil Y, Igoudjil W, Corvaisier M, Dessein AF, Vandomme J, Monte D, et al. Colon cancer cells escape 5FU chemotherapy-induced cell death by entering stemness and quiescence associated with the c-Yes/YAP axis. Clin Cancer Res 2014;20:837–46.
17. Corvaisier M, Bauzone M, Corfiotti F, Renaud F, El Amrani M, Monte D, et al. Regulation of cellular quiescence by YAP/TAZ and Cyclin E1 in colon cancer cells: Implication in chemoresistance and cancer relapse. Oncotarget 2016;7:56699–712.
18. Ameyar-Zazoua M, Rachez C, Souidi M, Robin P, Fritsch L, Young R, et al. Harel-Bellan A. Argonaute proteins couple chromatin silencing to alternative splicing. Nat Struct Mol Biol 2012;19:998–1004.
19. Mozzetta C, Pontis J, Fritsch L, Robin P, Portoso M, Proux C, et al. The histone H3 lysine 9 methyltransferases G9a and GLP regulate polycomb repressive complex 2-mediated gene silencing. Mol Cell 2014; 53:277–89.
20. Zhao B, Wei X, Li W, Udan RS, Yang Q, Kim J, et al. Inactivation of YAP oncoprotein by the Hippo pathway is involved in cell contact inhibition and tissue growth control. Genes Dev 2007;21:2747–61.
21. Zhang Y, Zolfaghari R, Ross CA. Multiple retinoic acid response elements cooperate to enhance the inducibility of CYP26A1 gene expression in liver. Gene 2010;464:32–43.
22. Dessein AF, Stechly L, Jonckheere N, Dumont P, Monté D, Leteurtre E, et al. Autocrine induction of invasive and metastatic phenotypes by the MIF-CXCR4 axis in drug-resistant human colon cancer cells. Cancer Res 2010;70:4644–54.
23. Muindi JR, Frankel SR, Huselton C, DeGrazia F, Garland WA, Young CW Jr, et al. Clinical pharmacology of oral all-trans retinoic acid in patients with acute promyelocytic leukemia. Cancer Res 1992;52:2138–42.
24. Simandi Z, Horvath A, Wright LC, Cuaranta-Monroy I, De Luca I, Karolyi K, et al. OCT4 acts as an integrator of pluripotency and signal-induced differentiation. Mol Cell 2016;63:647–61.
25. Kashyap V, Laursen KB, Brenet F, Viale AJ, Scandura JM, Gudas LJ. RARgamma is essential for retinoic acid induced chromatin remodeling and transcriptional activation in embryonic stem cells. J Cell Sci 2013;126: 999–1008.
26. Purton LE, Dworkin S, Olsen GH, Walkley CR, Fabb SA, Collins SJ, et al. RARgamma is critical for maintaining a balance between hematopoietic stem cell self-renewal and differentiation. J Exp Med 2006;203:1283–93.
27. Paramasivam M, Sarkeshik A, Yates JR 3rd, Fernandes MJ, McCollum D. Angiomotin family proteins are novel activators of the LATS2 kinase tumor suppressor. Mol Biol Cell 2011;22:3725–33.
28. Moleirinho S, Hoxha S, Mandati V, Curtale G, Troutman S, Ehmer U, et al. Regulation of localization and function of the transcriptional co-activator YAP by angiomotin. Elife 2017;6:e23966.
29. Stein C, Bardet AF, Roma G, Bergling S, Clay I, Ruchti A, et al. YAP1 exerts its transcriptional control via TEAD-mediated activation of enhancers. PLoS Genet 2015;11:e1005465.
30. Galli GG, Carrara M, Yuan WC, Valdes-Quezada C, Gurung B, Pepe-Mooney B, et al. YAP drives growth by controlling transcriptional pause release from dynamic enhancers. Mol Cell 2015;60:328–37.
31. Guo PD, Lu XX, Gan WJ, Li XM, He XS, Zhang S, et al. RARgamma down-regulation contributes to colorectal tumorigenesis and metastasis by derepressing the hippo-yap pathway. Cancer Res 2016;76:3813–25.
32. Zhou D, Zhang Y, Wu H, Barry E, Yin Y, Lawrence E, et al. Mst1 and Mst2 protein kinases restrain intestinal stem cell proliferation and colonic tumorigenesis by inhibition of Yes-associated protein (Yap) overabundance. Proc Natl Acad Sci U S A 2011;108:E1312–20.
33. Arnold SL, Kent T, Hogarth CA, Schlatt S, Prasad B, Haenisch M, et al. Importance of ALDH1A enzymes in determining human testicular retinoic acid concentrations. J Lipid Res 2015;56:342–57
34. Vidovic D, Huynh TT, Konda P, Dean C, Cruickshank BM, Sultan M, et al. ALDH1A3-regulated long non-coding RNA NRAD1 is a potential novel target for triple-negative breast tumors and cancer stem cells. Cell Death Differ 2020;27: 363–78.

AACR American Association for Cancer Research

Molecular Cancer Research

Cross-talk between YAP and RAR-RXR Drives Expression of Stemness Genes to Promote 5-FU Resistance and Self-Renewal in Colorectal Cancer Cells

Marjolaine Bauzone, Mouloud Souidi, Anne-Frédérique Dessein, et al.

Mol Cancer Res 2021;19:612-622. Published OnlineFirst January 20, 2021.